*Int. J. Morphol.,*
*41(4)*:1043-1052, 2023.

# Altered Chief Cell Morphology in the Gastric Gland of Streptozotocin-Diabetic Rats

## Morfología Celular Principal Alterada en la Glándula Gástrica de Ratas Diabéticas con Estreptozotocina

**Sani Baimai[1,2]; Sirinush Sricharoenvej[2]; Passara Lanlua[2] & Narawadee Choompoo[1]**

**BAIMAI, S.; SRICHAROENVEJ, S.; LANLUA, P. & CHOOMPOO, N.** Altered chief cell morphology in the gastric gland of streptozotocin-diabetic rats. *Int. J. Morphol., 41(4)*:1043-1052, 2023.

**SUMMARY:** Diabetes mellitus (DM) is a metabolic disorder with rising incidences worldwide. Gastric symptoms of DM have been reported, including nausea, vomiting, bloating, and epigastric pain. Moreover, acute to chronic gastritis and atrophic gastritis occur in DM can affect the chief cells of the gastric gland. Chief cells are vital because of their ability to digest and separate vitamin B12 from protein. Lack of vitamin B12 leads to impaired DNA synthesis and abnormal metabolism in red blood cells, and eventually leading to pernicious anemia. Furthermore, decreased vibratory and positional senses, numbness, ataxia with subacute combined degeneration, and dementia are present in pernicious anemic patients. Twenty-four male adult Sprague-Dawley rats were used in this study. The rats were divided into control (n = 12) and diabetic (n = 12) groups. The rats were further separated into two categories: short-term (4 weeks) and long-term (24 weeks) groups. DM model was induced by manually injecting intraperitoneally with streptozotocin in citrate buffer at a dose of 60 mg/kg body weight. The same amount of buffer was injected into the control group. After sacrifice, three regions of the stomach (the cardia, body, and pylorus) were dissected. Histopathology was performed by staining with toluidine blue. Image analysis was used to quantify the zymogen granule accumulation in chief cells. The data were compared between the control and DM rats in each period using Student's t-test. In addition, transmission electron microscopy (TEM) was also used to examine the ultrastructures. There was a significant decrease in the percentage of zymogen granules in DM rats. Under TEM, the destructions of mitochondria, rough endoplasmic reticulum, and Golgi apparatus in the DM rat were observed in the chief cells. In rats with uncontrolled diabetes, there is damage to the chief cells all over the area of the stomach, affecting digestion and malabsorption of vitamin B12. Therefore, this result helps clinicians recognize that diabetic patients with gastric symptoms may have hidden pernicious anemia.

**KEY WORDS Chief cells; Stomach; Zymogen granules; Streptozotocin; Ultrastructure; Rat.**

## INTRODUCTION

Diabetes mellitus (DM) is an increasing comorbidity of metabolic syndrome. There are many types of diabetes, including types 1 and 2, which are the most common among diagnosed patients (Sabatine, 2020). If the blood glucose level is not kept within the normal or acceptable range, the patient may inevitably have poor control of DM and consequently may suffer from complications. DM complications have been reported in the respiration, endocrine, and gastrointestinal systems, (Baimai *et al*., 2021; Chookliang *et al*., 2021; Lerkdumnernkit *et al*., 2022). Most diabetic patients with diabetic gastropathy (75 %) experience a variety of gastrointestinal symptoms, including abdominal bloating, nausea, vomiting, and epigastric pain (Krishnan *et al*., 2013). DM can also lead to gastritis in three phases. The first phase is acute gastritis which contains two steps: superficial erosions and mucosal erythema with edema. The second phase is chronic gastritis which causes depressed mucosal lesion appearances. The third phase is atrophic gastritis that gastric glandular cells are lost and replaced by fibrous tissue (Longo *et al*., 2013). It has been reported that the prevalence of vitamin B12 deficiency in DM occurs at 5.8–52 % (Kwape *et al*., 2021). Stomach gastritis occurs together with the incidence report of vitamin B12 deficiency in DM. That is probably related to the fact that DM causes damage to the glandular tissue and chief cells involved in the digestion of proteins to differentiate vitamin B12.

[1] Department of Anatomy, Faculty of Medical Science, Naresuan University, Phitsanulok, 65000, Thailand.
[2] Department of Anatomy, Faculty of Medicine Siriraj Hospital, Mahidol University, Bangkok, 10700, Thailand.

Received: 2023-04-05 Accepted: 2023-05-06

Generally, chief cells occupy the gastric gland in all regions, such as the cardiac gland, gastric gland proper, and pyloric gland. Chief cells produce and secrete pepsinogen and pepsinogen is activated by HCl from parietal cells into pepsin (an active enzyme) (Barrett *et al*., 2010; Costanzo, 2015). Pepsin can digest and isolate vitamin B12 from protein. Then, vitamin B12 binds with the R protein secreted from the salivary gland in the stomach; whereas in the small intestine, vitamin B12 binds with an intrinsic factor (IF) secreted from the parietal cells of the gastric gland. At the terminal ileum, IF releases vitamin B12 into intestinal cells. Finally, vitamin B12 binds to transcobalamin II and is transported to the liver via the portal vein (Barrett *et al*., 2010; Longo *et al*., 2013; Costanzo, 2015). Vitamin B12, or cobalamin, a cofactor of methionine synthase, has three major reactions. The first reaction is a conversion of methylmalonic acid to succinyl-CoA. The second reaction is the conversion of homocysteine to methionine. The third reaction is the conversion of methyl H4-folate to H4-folate (Barrett *et al*., 2010; Longo *et al*., 2013; Costanzo, 2015; Green *et al*., 2017). In DM patients, it was found that the stomach had diseases ranging from gastritis to atrophic gastritis (Krishnan *et al*., 2013; Longo *et al*., 2013). This condition inevitably affects the chief cell, resulting in cell damage, cell death, and decreased in cell number, which also affects the production and secretion of pepsinogen. Therefore, vitamin B12 cannot be collected and extracted from protein if the chief cell is deceased, dysfunction, or unable to break the protein. In DM, vitamin B12 deficiency can inhibit methionine synthase activity, increase methylmalonic acid, increase homocystinuria, and increase the folate trap (as methyltetrahydrofolate). In erythropoiesis, the folate trap can cause ineffective DNA synthesis of red blood cells (Barrett *et al*., 2010; Longo *et al*., 2013; Costanzo, 2015; Green *et al*., 2017). Hence, cytoplasm of red blood cell matures rather than the nucleus (ineffective erythropoiesis and macrocytosis). Finally, red blood cells are found as macro-ovalocytes, anioscytosis, and poikiocytosis causing megaloblastic anemia. Megaloblastic anemia is generated by many factors, such as folic acid deficiency and vitamin B12 deficiency. Due to a deficiency in vitamin B12, a condition known as pernicious anemia occurs when the body is unable to produce enough healthy red blood cells. Pernicious anemic patients have many signs and symptoms such as diminished vibratory and positional awareness, numbness, ataxia, subacute combined degeneration, and dementia (Barrett *et al*., 2010; Longo *et al*., 2013; Costanzo, 2015; Green *et al*., 2017).

Although there are many reports of diabetic chief cells, the histopathology and ultrastructure of chief cells and the proportion of zymogen granules in each region of the diabetic stomach (cardia, body, and pylorus) related to their functions have not been described. It is interesting to compare and determine the percentage of zymogen granules by using quantitative analysis. Moreover, the ultrastructural changes using transmission electron microscopy (TEM) of the chief cells in STZ-diabetic disease model in short and long periods were also investigated. This study provides an understanding of the percentage of zymogen granules and ultrastructural alterations of chief cells related to their functional impairments during DM progress. Furthermore, the present study raises awareness of GI complications as well as hematologic and neurologic complications to improve the quality of life in DM patients.

## MATERIAL AND METHOD

**Animal preparation.** Twenty-four male adult Sprague-Dawley rats, weighing 200–230 g, were used. They were 6–8 weeks old. The National Laboratory Animal Center at Mahidol University in Thailand provided the animals for all of the experiments. The animals were cared for according to the "Guide for the Care and Use of Laboratory Animals," which was approved by the Siriraj Animal Care and Use Protocol at Mahidol University in Thailand (COA No. 001/2564). Each was placed in a clean, isolated cage and treated according to a timetable (Baimai *et al*., 2021; Chookliang *et al*., 2021; Lerkdumnernkit *et al*., 2022). In addition, they had access to water and a typical lab meal during the experiment.

**STZ induction.** The animals were assigned to two groups at random to form STZ-induced diabetes and control groups. A single intraperitoneal injection of STZ at a dose of 60 mg/kg body weight in citrate buffer with a pH of 4.5 was delivered to 12 diabetic rats. Twelve rats in the age-matched control group received the same dosages of the buffer intraperitoneally (Baimai *et al*., 2021; Chookliang *et al*., 2021; Lerkdumnernkit *et al*., 2022).

**Diabetic confirmation.** Rat urine was checked to determine the presence of glucose. A blood sample that was also collected is used to evaluate the total blood glucose level. In this experiment, animals could be used if their overall blood glucose levels were less than 300 mg/dL and their urine glucose concentration was zero mg/dL. Urine and total blood glucose levels were tested following induction and before sacrifice (Baimai *et al*., 2021; Chookliang *et al*., 2021; Lerkdumnernkit *et al*., 2022). Daily body weight measurements were performed. For short- and long-term DM, all rats were divided into groups of four and twenty-four weeks, respectively.

**Study of the histopathology.** Before sacrifice, all rats were fasted for 12 hours and then anesthetized by halothane inhalation. 2.5 % glutaraldehyde in 0.1 M phosphate buffer solution (PBS) was manually applied to preserve the tissues after the perfusion with PBS (Baimai *et al*., 2021; Chookliang *et al*., 2021). The stomach was then removed, split open along the greater curve, and immersed overnight in the same fixative. After that, the stomach was surgically removed. Each area was recognized and then cut. TEM was used to process small stomach sections (1x1x1 mm3) that had been postfixed in 1 % osmium tetroxide in 0.1 M PBS (Baimai *et al.*, 2021; Chookliang *et al*., 2021). Toluidine blue was used to stain semithin sections (1-1.5 μm) from a Leica EM UC6 in Vienna, Austria, which were then analyzed under the LM for representative regions. Toluidine blue was also used to see the zymogen granules inside the chief cells.

**Quantitative approach.** Zymogen granules in chief cells were made as semithin toluidine-blue-stained slices, and their number was counted. For each of the 90 sections, the percentage of zymogen granules per region at 100x magnification was determined to measure the blue-stained zymogen granule depositions. Using Image J software, the percentage of zymogen granules in the chief cells was determined (National Institute of Mental Health, Bethesda, Maryland, USA).

**Research on ultrastructure.** The chosen embedding specimens were serially sliced at a thickness of 80–85 nm using an ultramicrotome. The serial sections were then stained with 1 % uranyl acetate and lead citrate (Baimai *et al.*, 2021; Chookliang *et al.*, 2021). The stomach ultrastructure was examined and captured on a camera using TEM (TECNI20, Phillips Electron Optics, Holland).

**Statistical assessment.** The mean and standard deviation (SD) of the data was calculated. Student's t-test was used to assess differences between independent groups (SPSS version 20.0 software, Inc., Chicago, IL, USA). At a p-value of 0.05, differences were determined to be significant.

## RESULTS

Diabetes symptoms such as polyuria, polydipsia, polyphagia, and generalized myopathy were observed in the DM rats. The symptoms of long-term diabetic rats were more severe than those of short-term diabetic rats. The majority of diabetic rats were lethargic, hypersomnia, and inactive. The glucose levels in urine and blood exceeded 500 mg/dL and 300 mg/dL, respectively. Before the sacrifice of rats, every rat was fasted for 12 hr. It was found that the control rats had no food residue at all. Only the DM rats had food residue with indigestible food inside their stomachs when the stomachs were opened.

**Histopathology and quantitative analysis of zymogen granules.** In short and long-term DM conditions, decreased zymogen granules were observed in all glands, such as the cardiac gland (Figs. 1B, 2B), gastric gland proper (Figs. 1D, 2D), and pyloric gland (Figs. 1F, 2F) when compared to the control group (Figs. 1A, 1C, 1E, 2A, 2C, 2E). When observing the size of zymogen granules in LM, it was found that the size of zymogen granules in diabetic rats was smaller than control rats in both short- and long-term periods (Figs. 1-2).

The percentage of zymogen granule accumulation was significantly decreased in both DM groups when compared to the age-matched control rats (Fig. 3A). In addition, the long-term diabetic rats had a significantly greater decrease in zymogen granule accumulation than short-term diabetes (Fig. 3B).

**Ultrastructures of the chief cells.** The structure for producing and secreting proteins found in their basal nucleus is a rough endoplasmic reticulum (rER). Several flattened rER in the basal area were well-developed, with extensive cisternae parallel to the cell axis (Figs. 4A, 4C, 4E, 5A, 5C, 5E). Large, electron-dense, membrane-bound secretory vesicles were found in zymogen granules (Figs. 4A, 4C, 4E, 5A, 5C, 5E). On the apical surface, zymogen granules were exocytosed. In addition, the apical surface was covered by many microvilli (Figs. 3A, 3C, 3E, 5A, 5C, 5E).

In short-term DM, the chief cell has a dilated and fragmented basal rER (Fig. 3F). Some apical variable size electron-dense or lucent granules and a basal oval euchromatin nucleus was observed (Figs. 3B, 3D, 3F); the chief cells of diabetic rats' stomachs had much smaller secretory granules (Figs. 3B, 3D, 3F). At high magnification, there were irregularly discontinued nuclear membranes (Fig. 3G) with heterochromatin nuclear clumping (Figs. 3G-H), damaged and fragmented rER (Figs. 3G-H), degenerated mitochondria (Figs. 3G-H), and numerous large vacuolar degenerations (Fig. 3G). Unidentified structures were observed (Figs. 3G-H). Nevertheless, a few small zymogen granules were present in degenerative chief cells (Fig. 3G), there were also found some huge zymogen granules in the chief cells (Figs. 3G-H).

In long-term DM, zymogen granules in chief cells were smaller than in short-term DM (Figs. 5B, 5D, 5F). In the degenerated chief cells, there were present some huge

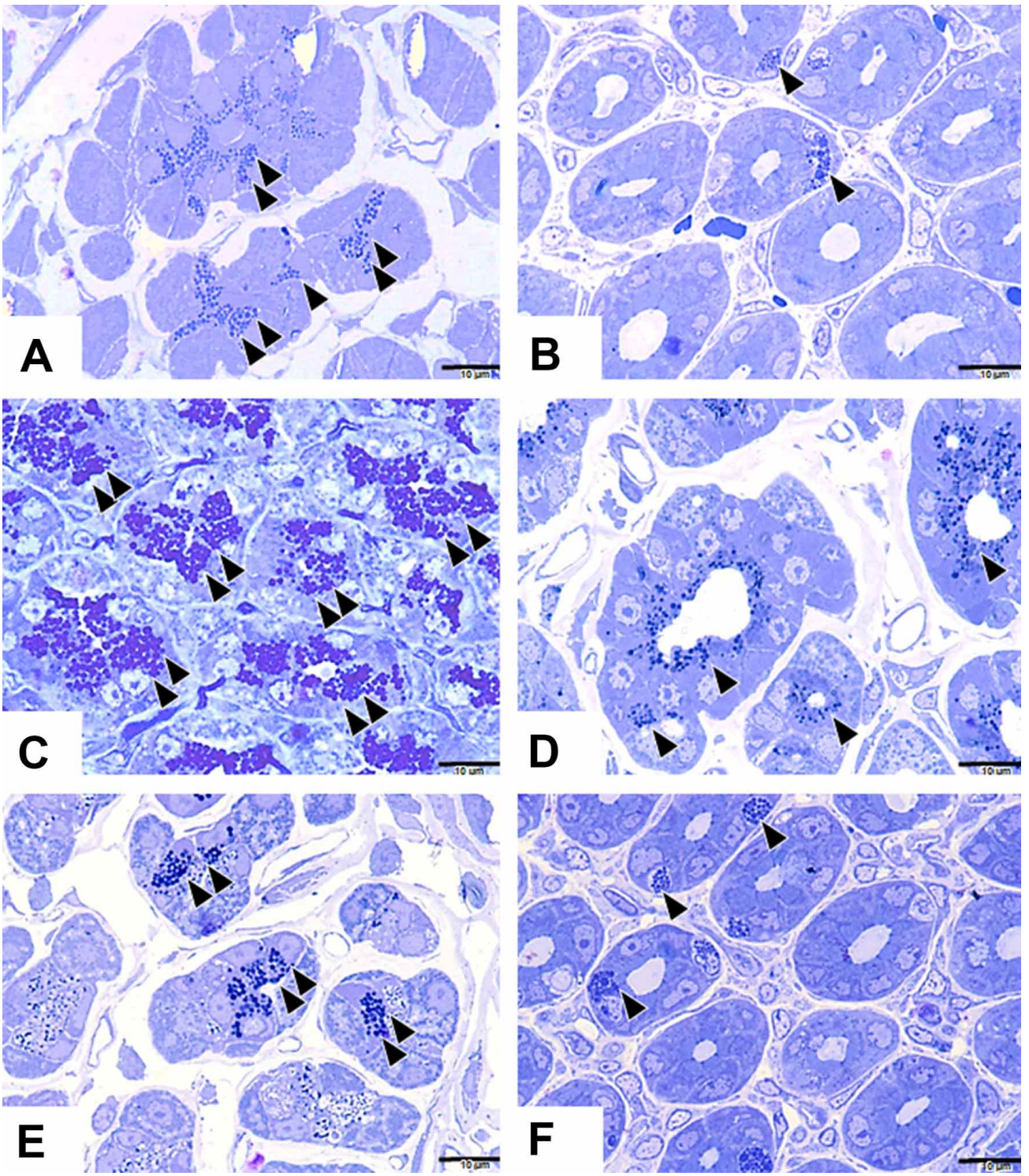


Fig. 1 Light micrographs of cardiac gland (A-B), gastric gland proper (C-D), and pyloric gland (E-F) of short-term control (A, C, E) and short-term diabetic (B, D, F) rats. Zymogen granules (black arrowheads). Toluidine blue staining. Scale bar = 10 μm.

zymogen granules (Figs. 5G-H). Shrinkage and destruction of chief cells were observed (Figs. 5D, 5F, 5H). Loss of cytoplasmic organelles in the cytoplasm was demonstrated (Figs. 5B, 5F, 5G). Nuclear heterochromatin clumping was

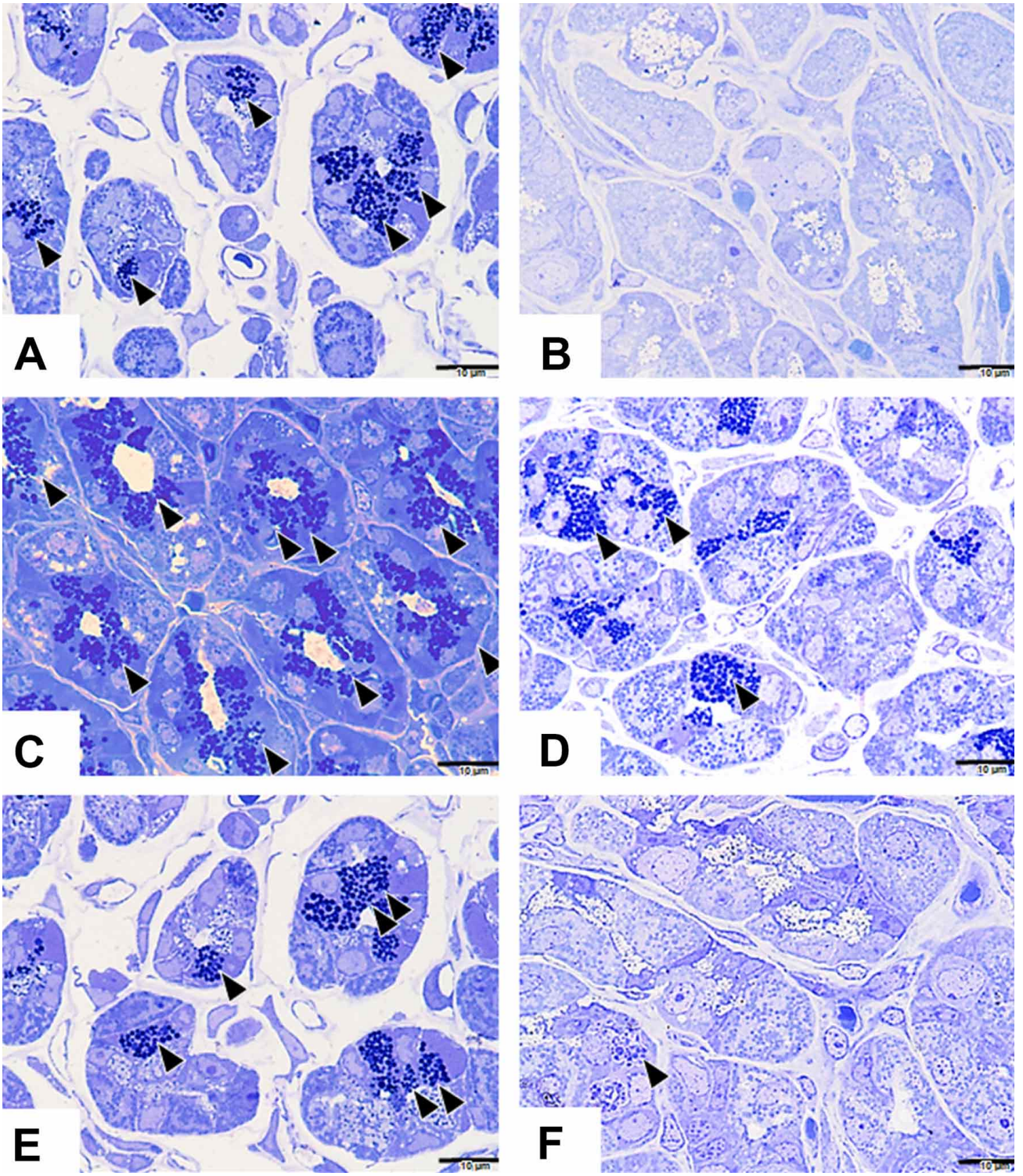


Fig. 2 Light micrographs of cardiac gland (A-B), gastric gland proper (C-D), and pyloric gland (E-F) of long-term control (A, C, E) and long-term diabetic (B, D, F) rats. Zymogen granules (black arrowheads). Toluidine blue staining. Scale bar = 10 μm.

exhibited (Figs. 5B, 5D, 5F, 5G, 5H). Vacuolar degeneration and a dilated rER of the chief cell were engulfed by macrophages (Fig. 5F). An electron-lucent area and unidentified structures were revealed (Figs. 5B, 5D).

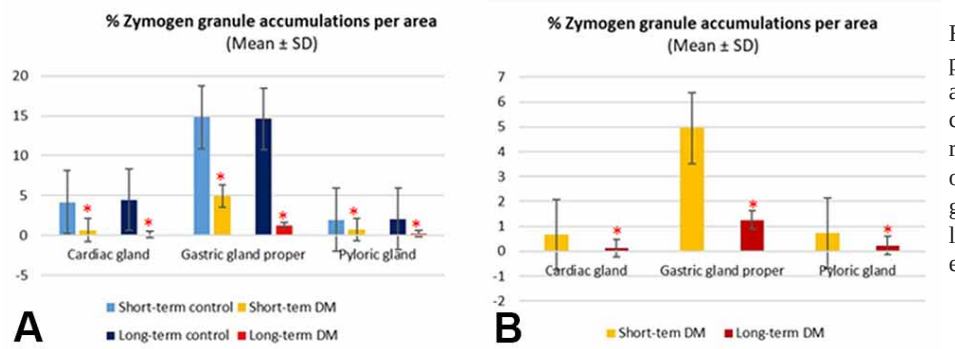


Fig. 3. A comparison of the percentage of zymogen granules per area in short- and long-term DM, compared to the age-matched control rats (A), in each gland. Comparison of the percentage of zymogen granules per area between short- and long-term DM in each gland (B), in each gland. Mean ± SD; * $p<0.05$

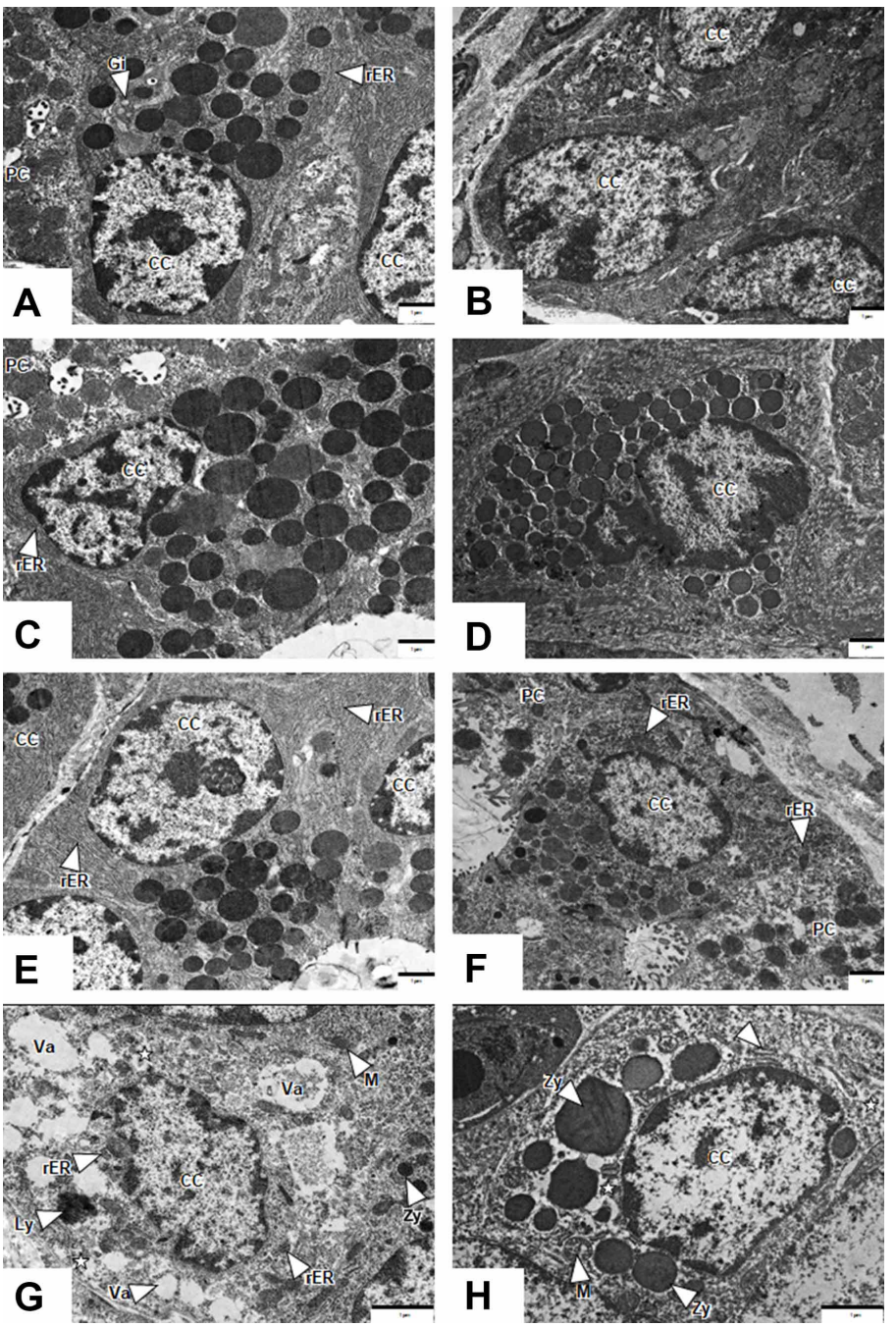


Fig. 4 Transmission electron micrograph of chief cells of cardiac gland (A-B), gastric gland proper (C-D), and pyloric gland (E-F) of short-term control (A, C, E) and short-term DM (B, D, F, G, H) rats. Parietal cell (PC); chief cell (CC); rough endoplasmic reticulum (rER); golgi complex (Gi); mitochondria (M); vacuole (Va); lysosome (Ly); larges zymogen granule (Zy); unidentified structures (white stars). Scale bar = 1 µm.

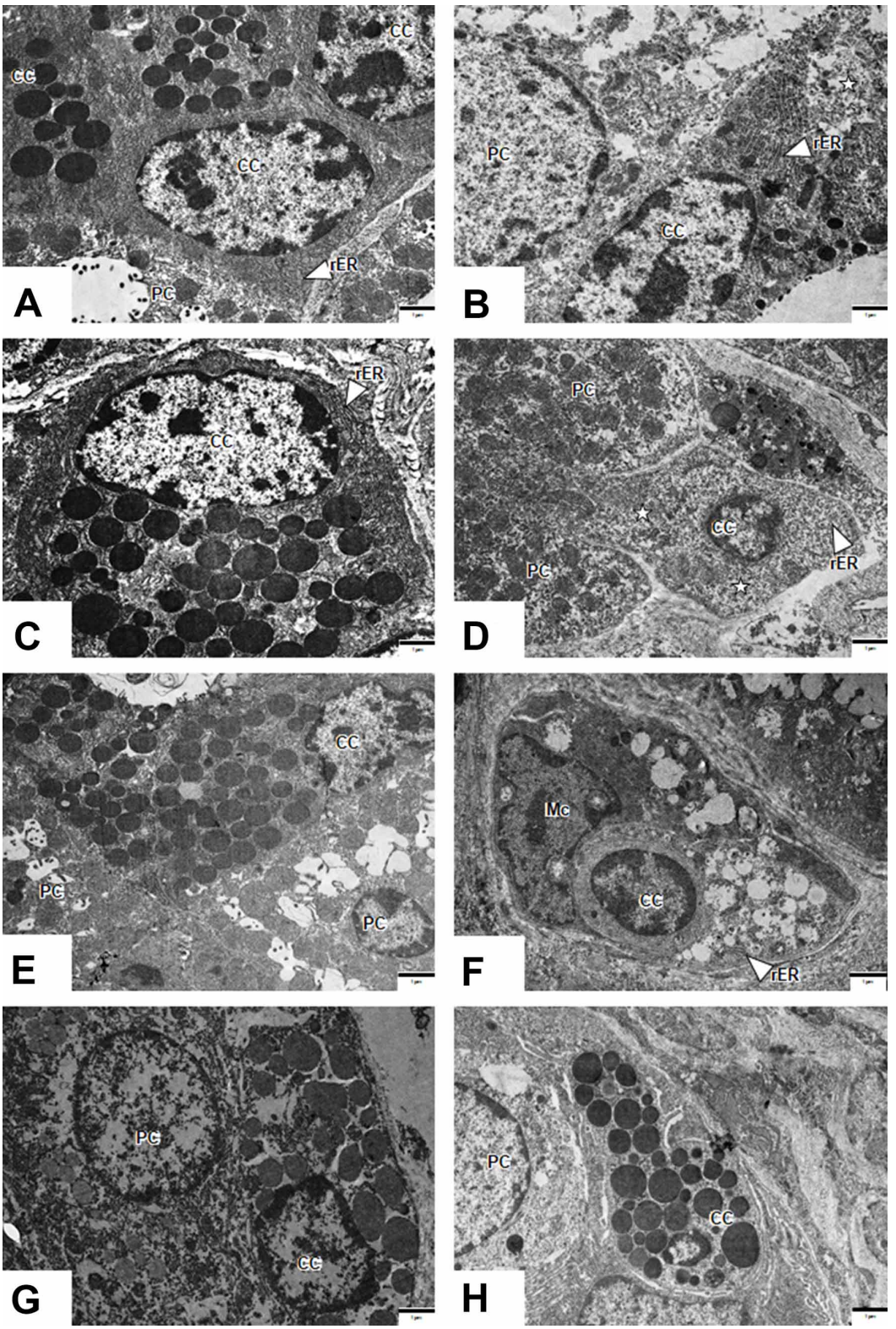


Fig. 5 Transmission electron micrograph of chief cells of cardiac gland (A-B), gastric gland proper (C-D), and pyloric gland (E-F) of long-term control (A, C, E) and long-term DM (B, D, F, G, H) rats. Parietal cell (PC); chief cell (CC); rough endoplasmic reticulum (rER); macrophage (Mc); unidentified structures (white stars). Scale bar = 1 μm.

## DISCUSSION

The diabetic signs and symptoms in this experiment were similar to the previous studies (Techarang *et al*., 2017; Baimai *et al*., 2021; Chookliang *et al*., 2021; Lerkdumnernkit *et al*., 2022). The residual and indigestible food were found only in DM rats after fasting for 12 h. There is evidence that people with diabetes have a lower density of myelinated vagus nerve fibers (Guo *et al*., 1987; Yu *et al*., 2019). The vagus nerve is also dysfunctional in diabetes patients with poor glycemic control (Guo *et al*., 1987; Yu *et al*., 2019). The vagus nerve supplies all gastric glands in the stomach. If the vagus nerve is destroyed, the nerve supply to the chief cells is reduced. As a result, destroyed chief cell ultrastructures and a decrease in zymogen granules were seen in the DM condition. It can imply that DM affects digestion in the stomach.

In DM rats, there were many vacuolar degenerations and destructive organelles with undetermined features. The results can be explained by the mechanism of diabetes as follows. The polyol pathway, which transforms circulatory glucose into sorbitol, uses aldose reductase and NADPH. The concentration of sorbitol then rises as a result of too much glucose in the blood. Afterwards, via the diffusion of water into the principal cells, the increase in intracellular fluid molarity and osmotic stress cause vacuolar degeneration in these cells (Yan, 2018; Ighodaro, 2018).

In a diabetic condition, the rER was markedly dilated and fragmented and damaged mitochondria were observed. The damage to mitochondria and rER in diabetes is characterized by DM pathology. As described above, a large amount of NADPH is consumed when excess glucose is converted to sorbitol. The synthesis of glutathione (GSH), which is a crucial cofactor, is needed for the conversion of NADPH to NADP+. The NADPH reduction caused by high blood glucose may impair GSH synthesis. GSH can stop damage to critical cellular components caused by reactive oxygen species (ROS) such as free radicals, peroxides, and lipid peroxides (Sandireddy *et al*., 2014; Volpe *et al*., 2018; Yaun *et al*., 2019). Therefore, a rise in ROS causes a decline in GSH. The sorbitol is oxidized to fructose by using sorbitol dehydrogenase (SDH), which creates NADH from NAD+. The elevated level of NADH leads to overwhelming ROS production from the mitochondrial electron transport chain. In a hyperglycemic state, NADH is overproduced and GSH is downregulated, which can promote ROS levels (Sandireddy *et al*., 2014; Volpe *et al*., 2018; Yaun *et al*., 2019). Subsequently, the upregulation of ROS is the cause of oxidative degradation of unsaturated fatty acids in lipid peroxidation, and then membrane damage of cells and organelles occurs via these processes (Sandireddy *et al*., 2014; Volpe *et al*., 2018; Yaun *et al*., 2019). After the membranes of cells and organelles are destroyed, extracellular ions and fluids influx into the cells and organelles, leading to organelles swelling with vacuolar degeneration and elevated intracellular calcium ions (Ca2+) in these cells. Moreover, lipid peroxidation causes mitochondrial dysfunction (Görlach *et al*., 2015; Yaun *et al*., 2019).

A reduced percentage of zymogen granule accumulation was observed in DM. Moreover, it was simpler to identify smaller secretory granules as zymogen granules under TEM. Under typical conditions, the protein-secreting chief cells are noticeable by TEM that the rERs are well-developed (Ross & Pawlina, 2011). In this experiment, the rER is damaged in diabetic circumstances, leading to fragmented rER in both short-term and long-term diabetes and resulting in zymogen production. In consequence, the zymogen granules were reduced and decreased. Therefore, it can be concluded that when rER is damaged, it cannot produce and reduced in size of zymogen granules, as can be seen in the experimental results, which are consistent in both quantitative analysis and ultrastructure.

Although, there were smaller sizes of zymogen granules in DM, the huge zymogen granules were also demonstrated in the degenerating DM chief cells. It can be explained by the DM mechanism. As mentioned above, ROS production during DM results in lipid peroxidation, which leads to the oxidative destruction of unsaturated fatty acids (Eizirik *et al*., 2008; Yaun *et al*., 2019). Cell and organelle membranes are destroyed. Intracellular Ca2+ leaks into the cytosol as a result of the rER's disrupted membrane (Eizirik *et al*., 2008; Yaun *et al*., 2019). Moreover, the proteolytic enzyme calpain-8, which cleaves the produced actin and myosin rings to transport granules for exocytosis, is active when intracellular Ca2+ levels are high (Görlach *et al*., 2015; Eizirik *et al*., 2008; Yaun *et al*., 2019). As a result, the zymogen granule transportation is blocked and inhibited. Thus, the zymogen granules of chief cells in the stomach of diabetic rats were identified as being smaller than those of normal rats, according to previous research (Bastaki *et al*., 2021). Furthermore, by the blocking exocytosis mechanism in DM, the degenerated chief cells in DM were presenting obstructed small zymogen granules that come together to form huge granules.

There were discontinuous and fragmented nuclear membranes with nuclear clumping of heterochromatin. These findings suggest apoptosis in DM. The increased ROS level from the polyol pathway during hyperglycemia directly generates BCI2-associated proteins (Bax) and BCI2 antagonist killer proteins (Bak), which are proapoptotic proteins (Krijnen *et al*., 2009; Ighodaro, 2018; Volpe *et al*., 2018; Tang *et al*., 2019). Next, the overexpressed Bax and Bak migrate from the cytoplasm to the outer membrane of the mitochondria and trigger mitochondrial outer membrane permeabilization by opening the mitochondrial permeability transition pore (Krijnen *et al*., 2009; Ighodaro, 2018; Volpe *et al*., 2018; Tang *et al*., 2019). Then, the cytochrome complex (Cyt C) is released from the mitochondrial intermembrane space to the cytosol. The binding between Cyt C and apoptotic protease activating factor-1 recruits procaspase-9 to activate the mature caspase-9, which is known as the apoptosome (Krijnen *et al*., 2009; Ighodaro, 2018; Volpe *et al*., 2018; Tang *et al*., 2019). The apoptosome induces apoptosis via caspase-3 activation to promote proteolytic enzymes, including endonuclease, protease, and lipase (Krijnen *et al*., 2009; Ighodaro, 2018; Volpe *et al*., 2018; Tang *et al*., 2019). The activation of endonucleases degrades chromosomal DNA, which leads to augmented heterochromatin condensation and a pyknotic nucleus. Proteases are responsible for breaking down organelles and the cytoskeleton. Lipase generates irregular cell and nuclear shapes via cell and organelle phospholipid membrane degradation (Krijnen *et al*., 2009; Ighodaro, 2018; Volpe *et al*., 2018; Tang *et al*., 2019). The regulation of these enzymes causes the nuclear membrane of the chief cells to rupture.

## CONCLUSION

The gastric glands, specifically the chief cells, are damaged when rats are given STZ to develop DM. The results showed a decrease in zymogen granules, including morphology and quantitative analysis, and damage to organelles in the cytoplasm of chief cells in every gland of the rats' stomach. The pepsinogen of chief cells can isolate vitamin B12 from protein-rich diets. Damage to the chief cells in DM impairs vitamin B12 absorption, resulting in pernicious anemia. Latent anemia in patients with poorly managed diabetes and gastrointestinal symptoms should be recognized by clinicians.

**ACKNOWLEDGEMENTS.** This research was supported by Chalermphrakiat Grant, Faculty of Medicine Siriraj Hospital, Mahidol University, Thailand.

**BAIMAI, S.; SRICHAROENVEJ, S.; LANLUA, P. & CHOOMPOO, N.** Morfología celular principal alterada en la glándula gástrica de ratas diabéticas con estreptozotocina. *Int. J. Morphol., 41(4)*:1043-1052, 2023.

**RESUMEN:** La diabetes mellitus (DM) es un trastorno metabólico con incidencia creciente a nivel mundial. Se han informado síntomas gástricos de DM, que incluyen náuseas, vómitos, distensión abdominal y dolor epigástrico. Además, la gastritis aguda a crónica y la gastritis atrófica que ocurren en la DM pueden afectar las células principales de la glándula gástrica. Las células principales son vitales debido a su capacidad para digerir y separar la vitamina B12 de las proteínas. La falta de vitamina B12 conduce a una síntesis de ADN deteriorada y un metabolismo anormal en los glóbulos rojos, lo que eventualmente conduce a una anemia perniciosa. Además, los pacientes con anemia perniciosa presentan disminución de los sentidos vibratorio y posicional, entumecimiento, ataxia con degeneración combinada subaguda y demencia. En este estudio se usaron 24 ratas Sprague-Dawley macho adultas. Las ratas se dividieron en grupos control (n = 12) y diabéticas (n = 12). Las ratas se separaron además en dos categorías: grupos a corto plazo (4 semanas) y a largo plazo (24 semanas). El modelo de DM se indujo inyectando manualmente por vía intraperitoneal estreptozotocina en tampón de citrato a una dosis de 60 mg/kg de peso corporal. Se inyectó la misma cantidad de tampón en el grupo control. Después del sacrificio, se disecaron tres regiones del estómago (cardias, cuerpo y píloro). La histopatología se realizó mediante tinción con azul de toluidina. El análisis de imágenes se utilizó para cuantificar la acumulación de gránulos de zimógeno en las células principales. Los datos se compararon entre las ratas control y DM en cada período utilizando la prueba t de Student. Además, se utilizó microscopía electrónica de transmisión (TEM) para examinar la ultraestructura celular. Hubo una disminución significativa en el porcentaje de gránulos de zimógeno en ratas DM. Bajo TEM, se observaron en las células principales las destrucción de las mitocondrias, del retículo endoplásmico rugoso y del complejo golgiense en la rata DM. En ratas con diabetes no controlada, hay daño en las células principales de toda el área del estómago, lo que afecta la digestión y la malabsorción de vitamina B12. Por lo tanto, este resultado ayuda a los médicos a reconocer que los pacientes diabéticos con síntomas gástricos pueden tener una anemia perniciosa oculta.

**PALABRAS CLAVE Células principales; Estómago; Gránulos de zimógeno; Estreptozotocina; Ultraestructura; Rata.**

## REFERENCES

Baimai, S.; Phanichkul, P.; Lanlua, P.; Niyomchan, A. & Sricharoenvej S. Modifications of adrenal gland ultrastructure in streptozotocin-induced diabetic model rats. *Int. J. Morphol., 39(1)*:109-15, 2021.

Barrett, K.; Brooks, H.; Boitano, S. & Barman, S. *Ganong's Review of Medical Physiology*. 23rd ed. New York, Mc Graw Hill, 2010.

Bastaki, S. M. A.; Amir, N.; Saeed, T. & Adeghate, E. Effects of diabetes mellitus on vitamin B12, pepsinogen and gastric intrinsic factor levels in rats. *Hamdan Med. J., 13(2)*:93-100, 2021.

Chookliang, A.; Lanlua, P.; Niyomchan, A. & Sricharoenvej, S. Small bronchiolar histopathological changes related to prolonged diabetes. *Int. J. Morphol., 39(2)*:371-7, 2021.

Costanzo, L. S. *BRS: Physiology*. 6th ed. Philadelphia, Wolters Kluwer, 2015.

Eizirik, D. L.; Cardozo, A. K. & Cnop, M. The role of endoplasmic reticulum stress in diabetes mellitus. *Endocr. Rev., 29(1)*:42-61, 2008.

Görlach, A.; Bertram, B.; Hudecova, S. & Krizanova, O. Calcium and ROS: A mutual interplay. *Redox Biol., 6*:260-71, 2015.

Green, R.; Allen, L. H.; Bjorke-Monsen, A. L.; Brito, A.; Gueant, J. L.; Miller, J. W.; Molloy, A. M.; Stabler, S.; Toh, B. H.; Ueland, P. M.; *et al*. Vitamin B12 deficiency. *Nat. Rev. Dis. Primers, 3*:17040, 2017.

Guo, Y. P.; McLeod, J. G. & Baverstock, J. Pathological changes in the vagus nerve in diabetes and chronic alcoholism. *J. Neurol. Neurosurg. Psychiatry, 50(11)*:1449-53, 1987.

Ighodaro, O. M. Molecular pathways associated with oxidative stress in diabetes mellitus. *Biomed. Pharmocother., 108*:656-62, 2018.

Krijnen, P. A. J.; Simsek, S. & Niessen, H. W. M. Apoptosis in diabetes. *Apoptosis, 14(12)*:1387-8, 2009.

Krishnan, B.; Babu, S.; Walker, J.; Walker, A. B. & Pappachan, J. M. Gastrointestinal complications of diabetes mellitus. *World J. Diabetes, 4(3)*:51-63, 2013.

Kwape, L.; Ocampo, C.; Oyekunle, A. & Mwita, J. C. Vitamin B12 deficiency in patients with diabetes at a specialised diabetes clinic, Botswana. *J. Endocrinol. Metab. Diabetes S. Afr., 26(3)*:101-5, 2021.

Lerkdumnernkit, N.; Sricharoenvej, S.; Lanlua, P.; Niyomchan, A.; Baimai, S; Chookliang, A.; Plaengrit, K.; Pianrumluk, S. & Manoonpol, C. The effects of early diabetes on duodenal alterations in the rats. *Int. J. Morphol., 40(2)*:389-95, 2022.

Longo, D. L.; Fauci, A. S.; Kasper, D. L.; Hauser, S. L.; Jameson, J. L. & Loscalzo, J. *Harrison's Manual of Medicine*. 18th ed. New York, McGrawHill, 2013.

Ross, M. H. & Pawlina, W. *Histology. A Text and Atlas with Correlated Cell and Molecular Biology*. 6th ed. Philadelphia, Wolters Kluwer, 2011.

Sabatine, M. S. Pocket Medicine. 7th ed. Philadelphia, Wolters Kluwer, 2020.

Sandireddy, R.; Yerra, V. G.; Areti, A.; Komirishetty, P. & Kumar, A. Neuroinflammation and oxidative stress in diabetic neuropathy: futuristic strategies based on these targets. *Int. J. Endocrinol., 2014*:674987, 2014.

Tang, D.; Kang, R.; Berghe, T. V.; Vandenabeele, P. & Kroemer, G. The molecular machinery of regulated cell death. *Cell Res., 29(5)*:347-64, 2019.

Techarang, T.; Lanlua, P.; Niyomchan, A.; Plaengrit, K.; Chookliang, A. & Sricharoenvej, S. Epidermal modification in skin of streptozotocin-induced diabetic rats. *Walailak J. Sci. Technol., 14(8)*:671-6. 2017.

Volpe, C. M. O.; Villar-Delfino, P. H.; dos Anjos, P. M. F. & Nogueira-Machado, J. A. Cellular death, reactive oxygen species (ROS) and diabetic complications. *Cell Death Dis., 9(2)*:119, 2018.

Yan, L. J. Redox imbalance stress in diabetes mellitus: Role of the polyol pathway. *Animal Model Exp. Med., 1(1)*:7-13, 2018.

Yaun, T.; Yang, T.; Chen, H.; Fu, D.; Hu, Y.; Wang, J.; Yuan, Q.; Yu, H.; Xu, W. & Xie, X. New insights into oxidative stress and inflammation during diabetes mellitus-accelerated atherosclerosis. *Redox Biol., 20*:247-60, 2019.

Yu, Y.; Hu, L.; Xu, Y.; Wu, S.; Chen, Y.; Zou, W.; Zhang, M.; Wang, Y. & Gu, Y. Impact of blood glucose control on sympathetic and vagus nerve functional status in patients with type 2 diabetes mellitus. *Acta Diabetol., 57(2)*:141-50, 2019.

Corresponding author:
Narawadee Choompoo, Ph.D.
Department of Anatomy
Faculty of Medical Science
Naresuan University
Phitsanulok 65000
THAILAND

E-mail: narawadeec@nu.ac.th